Article

Organic Petrology and Thermal Maturity of Dispersed Organic Matter from the Ramalhal-1 Well (Lusitanian Basin, Portugal)

Paula Alexandra Gonçalves [1,*] , **João Graciano Mendonça Filho** [2] **and Deolinda Flores** [1]

1   Instituto Ciências da Terra-Polo, Departamento de Geociências, Ambiente e Ordenamento do Território, Faculdade de Ciências, Universidade do Porto, Rua Campo Alegre 687, 4169-007 Porto, Portugal; dflores@fc.up.pt
2   Laboratório de Palinofácies & Fácies Orgânica (LAFO), Departamento de Geologia, Instituto de Geociências, Universidade Federal do Rio de Janeiro, Rio de Janeiro 21941-916, Brazil; graciano@geologia.ufrj.br
*   Correspondence: paula.goncalves@fc.up.pt

Abstract: Organic petrology is an important tool used to characterize dispersed organic matter (DOM) in sediments and sedimentary rocks, and to assess its thermal maturity. This study was carried out on 33 cutting samples (Middle-Upper Jurassic) from the Ramalhal-1 well to characterize the particulate organic matter and to evaluate its thermal maturity. The samples were submitted to optical petrography analysis (reflected white and blue incident lights) and the mean random reflectance was measured. Microscopic observations revealed a low DOM content, characterized by the predominance of macerals of the inertinite group (including charcoal), followed by solid bitumen. Huminite/vitrinite is usually small in size and quantity. Liptinite macerals were also present, represented by sporinite, cutinite, liptodetrinite and rare bituminite. A type III-IV kerogen was defined for the Ramalhal-1 sequence. Huminite/vitrinite mean random reflectance varied between 0.38% and 0.75%, pointing to an immature-to-mature stage of the organic matter. Multi-populations of solid bitumen occurred in almost all the samples, filling voids and fractures in the inorganic materials (mainly carbonates). The bitumen populations were quite heterogeneous, concerning both the optical characteristics and distribution, displaying different thermal maturities. No relationship between vitrinite and bitumen reflectance was established, indicating that these bitumens were not generated in situ.

Keywords: organic petrology; charcoal; huminite/vitrinite reflectance; bitumen reflectance

1. Introduction

Organic petrography is an important tool used to characterize the organic matter (OM) present in sedimentary sequences (e.g., [1–3]). Optical microscopy in reflected white light (RWL), fluorescence mode (FM) and transmitted white light has been demonstrated to be useful for assessing the type of organic matter associated with different paleoenvironments and for determining the thermal maturity reached by the organic matter during its geological evolution [1,3–9], among others. In addition, reflected microscopy may reveal the relationships between organic and inorganic matter that cannot be directly obtained by, for example, geochemical analyses.

In recent years, petrographic and geochemical studies have been carried out to characterize dispersed organic matter (DOM) in sediments from the Lusitanian Basin (Portugal), from both well and outcrop samples (e.g., [6–8,10,11]), to determine the occurrence and preservation of OM and to define its palaeodepositional environment, as well as to identify its potential source rocks and assess the degree of thermal evolution. Nevertheless, most petrographic studies relied on palynofacies analysis (transmitted microscopy), and maturity assessments were usually based on geochemical data, such as T_{max} or biomarker ratios (e.g., [6–8,11]). The combination of organic petrography and vitrinite reflectance measurements with geochemical analyses is advantageous for achieving more accurate

estimations/interpretations of the maturity level. However, in the case of the Lusitania Basin, geochemical parameters can often be ambiguous, not allowing for a correct thermal maturity assessment (e.g., [6,12]).

The present study aims: (i) to characterize, through organic petrography analysis under reflected white and blue incident lights, the dispersed organic matter present in a Middle-Upper Jurassic sedimentary succession from the Ramalhal-1 well; (ii) to assess the OM thermal maturity based on the huminite/vitrinite reflectance; (iii) to establish the relationship between huminite/vitrinite reflectance and bitumen reflectance (when present); and (iv) to discuss the possible impact of the presence of solid bitumen on the geochemical parameters presented by Gonçalves et al. [6].

2. Previous Work

Palynofacies and geochemical data of Ramalhal-1 well were published by Gonçalves et al. [6] and are summarized below. Transmitted microscopy, i.e., the palynofacies analysis, revealed the presence of the three main groups of kerogen- phytoclast, amorphous and palynomorph - plus solid bitumen, with a predominance of the phytoclast group. Within this group, non-opaque phytoclasts prevail relative to opaque phytoclasts, showing different degradation degrees. Cuticles and membranes were also observed. The amorphous group was represented by phytoplankton-derived OM, bacterial-derived OM, higher plant-derived OM and resin. In some cases, the amorphous OM was oxidized and revealed a dark color, in both transmitted white light and fluorescence mode. Regarding the palynomorph group, the major contribution was from the sporomorph subgroup, mainly spores of different species of plants. Freshwater palynomorphs (*Botryococcus)*, marine palynomorphs (dinocysts) and zoomorphs (foraminifera test-linings) were identified in a restricted number of samples (Oxfordian-Bathonian?). Geochemical data indicate a low to poor organic carbon content (mean value of 0.88 wt.%), and the modified van Krevelen plot of HI versus OI suggests a type III kerogen (continental origin). In contrast, biomarker data suggest a combination of continental and marine organic matter, except for the Lourinhã Formation, where the contribution is solely continental. The maturity level was established by T_{max} of pyrolysis and some biomarker ratios, such as $C_{32}22S/(22S + 22R)$ hopanes, $C_{29}20S/(20S + 20R)$ steranes and $C_{29}\beta\beta/(\alpha\alpha + \beta\beta)$ steranes, suggesting an immature to early-mature stage for the organic matter.

3. Brief Geological Background

The Lusitanian Basin (Figure 1A) is a sedimentary basin of Mesozoic age, located on the western part of the Iberian Peninsula. Its geodynamic fits into the context of the Pangea fragmentation, which triggered the opening of the North Atlantic [13]. The Ramalhal-1 well was drilled in the central sector of the Lusitanian Basin, at the Bombarral sub-basin. The Bombarral sub-basin (Figure 1B) corresponds to a salt withdrawal structure flanked by diapiric structures [14,15]. This sub-basin is separated from the Arruda and Turcifal sub-basins by a 70 km long northeast-to-east-trending structural lineament, the Torres Vedras-Montejunto lineament. In this sub-basin, early Jurassic units show evidence of halokinesis [16].

The Ramalhal-1 well crossed lithologies (Figure 1C) whose ages fall within the temporal interval between the Bathonian(?) and the Tithonian, recording an important basin-wide disconformity and a stratigraphic gap in the transition between the Middle and the Upper Jurassic. The Brenha Formation (informal unit; Pliensbachian to Callovian) is characterized by fossiliferous and/or bioturbated marls, marly limestones [17] and compact limestones [13,18], sometimes interbedded with shales in some sites of the Lusitanian Basin (e.g., [18–20]). This formation corresponds to a deep-marine carbonate ramp [13,17], where deposition occurred below storm waves, sometimes under anoxic conditions [14–17]. The Montejunto deposition occurred from Middle to Late Oxfordian in a shallow marine carbonate platform environment, with the sporadic deposition of clay resulting in the formation of micritic and compact limestones interbedded with marls [13]. The deposition

of the Abadia Formation (Kimmeridgian) testifies to an increase in siliciclastic input in submarine fans and prograding slope environment sedimentation [18], and is composed of marls interbedded with coarse sandstones and rare limestone levels [13,18]. Finally, the Lourinhã Formation (Tithonian) is characterized by sandstones interbedded with conglomerates and marly limestones [13] resulting from a fluvial-deltaic environment interfering with marginal marine shales [18].

Figure 1. Location map of (**A**) Lusitanian Basin and (**B**) Ramalhal-1 well. (**C**) Simplified stratigraphic column of Ramalhal-1 well. AF: Aveiro Fault; NF: Nazaré Fault; TF: Tagus Fault; GF: Grândola Fault (modified from Gonçalves et al. [6]).

4. Materials and Methods

4.1. Samples

Thirty-three samples were collected from Ramalhal-1 well, drilled in the onshore of the Lusitanian Basin, providing a Bathonian(?)-Tithonian sedimentary sequence (Figure 1C). The lithological data was gathered from the geological report (available upon request from the DGEG-Direção Geral de Energia e Geologia, Lisbon, Portugal). A summary of the lithologies crossed by the studied well is presented in Table 1.

Table 1. Summary of the lithologies crossed by Ramalhal-1 well (data from Ramalhal-1 geological report).

Formation	Age	Depth (m)	Number of Samples	Lithologies
Lourinhã	Tithonian	0–1024	6	Fine to medium-grained sand with beds of red clay (on top); red clay beds of coarse to medium-grained sandstone and marl; marl intercalated with fine to medium-grained sandstone.
Abadia	Kimmeridgian	1024–2027	7	Grey marl interbedded by layers of fine to medium-grained sandstone and limestone. On the top, thin layers of oolitic limestone.
Montejunto	Oxfordian	2027–3190	16	Reef limestone with interbedded grey-brown compact limestone (on top). Compact limestone with calcite layers.
Brenha	Callovian-Bathonian(?)	3170–3521	4	Compact limestone with interbedded oolitic limestone and thin layers of calcite.

4.2. Methodology

Optical petrography was performed on 33 whole rock polished blocks prepared according to standard procedures [21], and the mean random reflectance of huminite/vitrinite and solid bitumen (when present) were measured according to ASTM D7708 standard [22], using a Leica DM4000 microscope equipped with a Discus-Fossil system, resorting to a 50× oil immersion objective. The microscope was calibrated with yttrium, aluminum, garnet (YAG; 0.905% R_r) and an optical black (zero) standards. The classification of the organic matter followed the ICCP System 1994 [23–26] and Flores and Suárez-Ruiz [27].

5. Results

Organic petrographic analysis from samples collected in the Ramalhal-1 well reveal a low content of dispersed organic matter, as already reported by Gonçalves et al. [6]. Although a mineralogical study was not carried out, some mineralogical particularities were observed in the Ramalhal-1 samples. Ramalhal-1 corresponds to a carbonate-siliciclastic sequence. The organic matter is usually associated with the siliciclastic fraction, except for some bitumen populations that are associated with the carbonate fraction. Pyrite is common throughout the sequence, mainly in the framboidal form, and often associated with organic matter (Figure 2B,C,I). Oolites are common in the Abadia Formation, sometimes being large (Figure 2L). They were also occasionally observed in samples from Brenha and Montejunto formations. Rhombohedral dolomite and calcite were distinguished, mainly in the Brenha samples.

Macerals of the inertinite group (Figure 2A–C) are, by far, the most common type of primary organic components of the studied sequence, being present in all samples. Within the inertinite group, structured tissues (fusinite and semifusinite) and fine detrital fragments (inertodetrinite) were observed. Some inertinite particles showed devolatilization pores (Figure 2C), possibly related to natural pyrolysis (i.e., wildfires). Huminite/vitrinite was present in most of the samples, usually small in size, and its mean random reflectance ranged from 0.38% to 0.75% R_r (Table 2). In one sample from the Abadia Formation (1800 m of depth), the presence of colonies of heterotrophic bacteria on plant tissues was observed (Figure 2H). These bacteria are responsible for attacking terrestrial humic material, leading to the production of amorphous material. In some samples of the Lourinhã Formation, large huminite particles (Figure 2J) were observed, which exhibited a yellow-orange fluorescence color and presented reflectance values around 0.20–0.30% R_r. This type of particle predominates in the sample at 600 m depth.
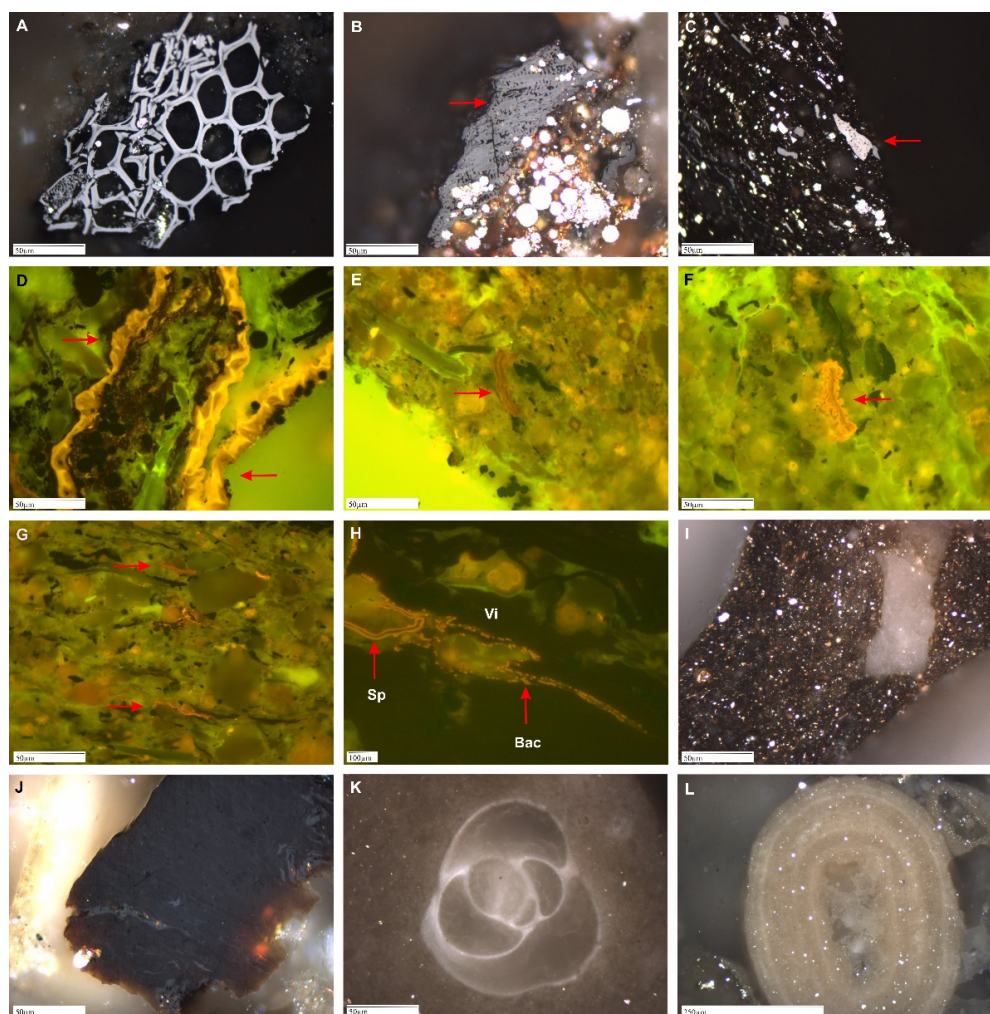
Figure 2. Photomicrographs of some petrographic features from Ramalhal-1 samples under reflected white light (**A**–**C**,**I**–**L**) and fluorescence mode (**D**–**I**). (**A**) Fusinite (1350 m depth); (**B**) semifusinite (2650 m depth); (**C**) inertodetrinite with devolatilization pores (3100 m depth); (**D**) cutinite (2650 m depth); (**E**,**F**) sporinite (1350 m and 1200 m depth, respectively); (**G**) liptodetrinite (3175 m depth); (**H**) bacteria (Bac) involving a vitrinite (Vi) particle and sporinite (Spo) (1800 m depth); (**I**) mineral-bituminous groundmass (2150 m depth); (**J**) huminite with suppressed reflectance (600 m depth); (**K**) carbonate carapace of foraminifera (2725 m depth); (**L**) oolite (1050 m depth).

Macerals of the liptinite group were also observed, represented by sporinite, cutinite, liptodetrinite and rarely bituminite. Some mineral-bituminous groundmass areas (Figure 2I), sometimes pyrite rich, were observed in carbonate-poor samples. Sporinite (Figure 2E,F,H) was present in all the samples, exhibiting a fluorescence color, which varied from yellow to brownish-orange. Big and ornamented spores were distinguished in Abadia and Montejunto formations (Figure 2F) as well as pollen grains of the genus *Classopollis* and sporangium. Large cutinite particles (Figure 2D), sometimes with the innermost part of the epiderm preserved, exhibited an intense yellow fluorescence color.

Secondary products, in the form of solid bitumen/pyrobitumen (Figure 3), were identified throughout the sequence, being more abundant in the Abadia Formation (Table 2). The bitumen shape varied according to the shape of the fractures and pores that it fills. Disseminated solid bitumen in the mineral matrix was also observed in some samples. Optical features, such as color in reflected and blue incident lights, morphology and reflectance, allowed for the differentiation of four populations of bitumen, identified as B1

to B4. The distribution of the different bitumens along the Ramalhal-1 sequence was not homogeneous (see Table 2).

Table 2. Mean random reflectance data of huminite/vitrinite and solid bitumen from Ramalhal-1 samples.

Formation	Depth (m)	Lithology	VR_r	Stdev (n)	$B1R_r$	Stdev (n)	$B2R_r$	Stdev (n)	$B3R_r$	Stdev (n)	$B4R_r$	Stdev (n)
Lourinhã	150	Clay										
	300	Clay	0.38	(1)								
	450	Clay	0.41	(1)	1.10	0.10 (12)						
	600	Sandstone	0.45	0.04 (20)								
	750	Marl	0.46	0.10 (9)	1.14	0.03 (5)			0.57	0.06 (4)		
	900	Marl	0.47	0.05 (15)	1.14	0.04 (2)			0.47	0.08 (4)		
Abadia	1050	Limestone	0.48	0.08 (5)			0.36	0.06 (9)	0.50	0.05 (9)		
	1200	Marl	0.47	0.04 (26)			0.41	0.07 (33)	0.68	0.05 (10)		
	1350	Marl	0.48	0.07 (34)			0.40	0.04 (16)	0.57	0.06 (9)		
	1500	Sandstone	0.50	0.07 (31)	1.08	0.13 (4)	0.44	0.04 (13)	0.65	0.09 (63)		
	1650	Marl	0.51	0.04 (13)	1.05	0.11 (44)	0.45	0.04 (3)	0.57	0.09 (8)		
	1800	Marl	0.58	0.04 (4)	1.00	0.07 (43)	0.51	0.05 (4)	0.72	0.06 (62)		
	1950	Marl	0.52	0.04 (8)	1.03	0.11 (28)	0.45	0.05 (4)	0.70	0.06 (9)		
Montejunto	2050	Limestone			1.03	0.11 (25)	0.50	0.06 (4)	0.70	0.06 (5)		
	2125	Limestone										
	2200	Limestone	0.61	0.03 (5)	1.09	0.10 (7)			0.64	0.06 (5)		
	2275	Limestone	0.64	0.02 (2)	1.08	0.03 (2)			0.65	(1)		
	2350	Limestone	0.66	0.09 (10)	1.10	0.15 (18)			0.65	0.10 (9)		
	2425	Limestone	0.67	0.07 (7)	1.20	0.16 (13)						
	2500	Limestone	0.68	0.08 (2)								
	2575	Limestone	0.68	0.10 (3)	1.15	0.16 (15)			0.62	0.06 (5)		
	2650	Limestone	0.69	0.07 (10)	1.18	0.11 (10)						
	2725	Limestone	0.68	0.04 (7)	1.20	0.12 (5)						
	2800	Limestone	0.69	0.06 (4)							2.31	0.22 (3)
	2875	Limestone	0.69	0.07 (18)							2.34	0.18 (17)
	2950	Limestone	0.68	0.03 (3)							2.35	0.16 (39)
	3025	Limestone	0.66	0.08 (2)	1.22	0.02 (2)					2.45	0.18 (45)
	3100	Limestone	0.70	0.07 (4)	0.97	0.01 (2)					2.37	0.15 (12)
	3175	Limestone	0.71	0.07 (8)	1.23	0.08 (2)					2.41	0.28 (10)
Brenha	3250	Limestone	0.71	0.05 (5)					0.64	(1)	2.40	0.22 (29)
	3325	Limestone	0.72	0.08 (13)	0.93	0.09 (8)			0.73	0.03 (4)	2.32	0.22 (17)
	3400	Limestone	0.74	0.06 (5)							2.33	0.20 (23)
	3475	Limestone	0.75	0.06 (9)	1.19	0.01 (2)					2.54	0.17 (72)

VR_r: huminite/vitrinite mean random reflectance (%); Stdev: standard deviation (%); *n*: number of measurements; $B1R_r$: population B1 mean random reflectance (%); $B2R_r$: population B2 mean random reflectance (%); $B3R_r$: population B3 mean random reflectance (%); $B4R_r$: population B4 mean random reflectance (%).
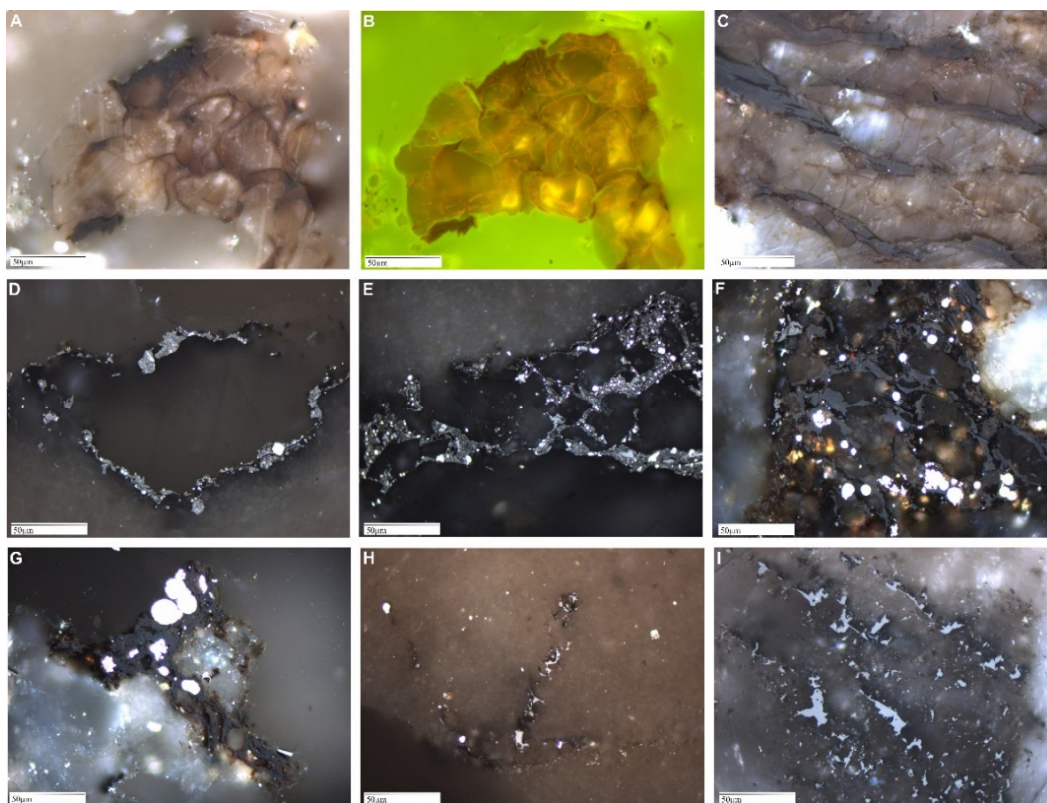
Figure 3. Photomicrographs of solid bitumen aspects from Ramalhal-1 samples under reflected white light (**A**,**C**–**I**) and fluorescence mode (**B**). (**A**–**C**) Solid bitumen B2 (600 m depth); (**D**,**E**) solid bitumen B1 (3325 m and 3475 m depth, respectively); (**F**,**G**) solid bitumen B3 (1500 m depth); (**H**,**I**) solid bitumen B4 (2950 m and 3400 m depth, respectively).

Population B1 was observed in all the formations, but its occurrence was not detected in all samples. This bitumen was optically isotropic and had a granular aspect, but it was possible to find some flat surfaces to perform reflectance measurements (Figure 3D–F). It had a grey color (under RWL) and showed a brownish fluorescence color. Sometimes it filled small voids, making it impossible to measure the reflectance. The bitumen presented features similar to solid bitumen A (grey color in RWL, brownish fluorescence, irregular surface and brittle aspect) identified by Gonçalves et al. [28] in the Arruda sub-basin (Lusitanian Basin). Population B2 was the least frequent bitumen, only detected in the Lourinhã and Montejunto formations (in the topmost sample). This bitumen has a flat surface, a homogeneous and viscous appearance and is usually associated with limestones. Under RWL, it had a brownish-grey to grey color (Figure 3A,C) and exhibited a yellow to brownish fluorescence color (Figure 3B). Population B3 was present in all samples from the Abadia Formation and some samples from the Montejunto and Brenha formations (see Table 2) being, sometimes, the dominant solid bitumen population. It had a dark grey color (under RWL; Figure 3F,G) and exhibited orange-to-brownish fluorescence. A similar bitumen had already been identified by Pereira et al. [10] in Lower Jurassic samples. Population B4 had smooth and easy polishing surfaces, a mosaic structure and was slightly anisotropic. It was a light-grey color and did not exhibit fluorescence color (Figure 3H,I). Similar bitumen features were also observed in the Arruda sub-basin (solid bitumen C) [28]. This type of bitumen prevailed in the Brenha Formation and in the bottom half of the Montejunto Formation (Table 2).

The mean random reflectance of the different solid bitumen populations was measured in 21 samples and the data are summarized in Table 2. It is noted that most samples present two or more solid bitumen populations. The mean random reflectance of the solid bitumen varied between: (i) 0.93% and 1.23%R_r for B1; (ii) 0.36% and 0.51%R_r for B2; (iii) 0.47% and 0.73%R_r for B3; and 2.31% and 2.54%R_r for B4.

6. Discussion

6.1. Organic Matter Characterization

The organic components observed in Ramalhal-1 samples included primarily inertinite, followed by liptinite (mainly sporinite and cutinite) and minor vitrinite (except for the Abadia Formation), indicating a terrestrial origin of the organic matter, typical of a proximal depositional environment. In the case of Brenha, the deposition occurred in a less proximal and oxidized environment [6]. The predominance of inertinite macerals throughout the Ramalhal-1 sedimentary sequence, sometimes with features of charcoal, evidences a type III-IV kerogen and corroborates data regarding palynofacies and Rock-Eval pyrolysis from Gonçalves et al. [6].

Inertinite macerals can originate from fine detrital fragments or tissues of fungi or higher plants, where the structural details of various stages of compaction or fracturing, including charcoal, can be seen. Charcoal is mainly classified as a fusinite maceral within the inertinite group; however, some semifusinite and inertodetrinite macerals may also be associated with wildfires [24]. On a global scale, the formation of charcoal is affected by the atmospheric oxygen concentrations, with paleoclimate conditions also playing a role in fire occurrence [29,30]. The concentration of O_2 has been varied throughout geological time, and almost the entire Jurassic is considered to have been a period of low oxygen concentration (approximately 13.5–16%; [31] and, consequently, less prone to fire occurrence, e.g., [32,33]). According to Uhl et al. [34], the frequency of paleofires during the Kimmeridgian was low, probably due to the low O_2 concentration, and its occurrence was associated with areas with seasonal climate conditions. Belcher and McElwain [35] established that the minimum atmospheric O_2 concentration required for ignition and sustained combustion, and, consequently, the formation of charcoal, is approximately 15%, although Chaloner [32] proposed a lower value of approximately 13%. Even though charcoal was present in all formations, the occurrence of large fusinite particles, with well-defined cell walls (Figure 2A) associated with inertodetrinite, showing devolatilization pores (Figure 2C), are mainly observed in the Kimmeridgian-Tithonian interval. Devolatilization pores in organic matter are related to the release of volatiles from the particles upon burning [36], as a result of the sudden and punctual heating associated with the intrusion of igneous rocks [37–40], which would produce a thermal perturbation easily recognized in the maturity profile, or the action of forest fires [41]. As there is no evidence of magmatic activity in this area of the Lusitanian Basin [13], the presence of particles with the charcoalification aspect associated with large fusinite particles suggests an environment that was prone to the occurrence of wildfires, possibly due to hot and dry paleoclimatic conditions [3] and an availability of atmospheric O_2 [42]. The presence of sporinite, both spores (sometimes big and ornamented; Figure 2F) and *Classopollis* pollen grains also confirms this assumption. These semi-arid conditions occurred seasonally in the Lusitanian Basin, having been identified, for example, during the Sinemurian [11], the Middle-Late Jurassic disconformity [17] and the Upper Jurassic [43]. The proximal depositional environment established for the Kimmeridgian-Tithonian samples by Gonçalves et al. [6] is supported by this study.

Large huminite particles, reported for the Lourinhã Formation, were isolated from the mineral matrix and, according to Gonçalves et al. [6], are related to the presence of perhydrous coal. Perhydrous coal in the Upper Jurassic of the Lusitanian Basin has already been reported by Costa et al. [44]. The reflectance of these particles (between 0.20–0.30%R_r) is suppressed relative to the reflectance of the primary huminite population (around 0.45%R_r). This suppression in reflectance can result from both the presence of in situ resinous substances [44–46] as well as the enrichment in hydrogen-rich substances, which can be related to the absorption of hydrocarbons and bituminous products present in the sediments or ones that migrated from older rocks in the sedimentary basin (e.g., [44,47–51]). The identification of perhydrous coal should be treated with caution when dealing with the thermal maturity assessment of the Lourinhã Formation.

6.2. Thermal Maturity of Organic Matter

Huminite/vitrinite reflectance (from organic petrography) and T_{max} values (from Rock-Eval pyrolysis) are two of the most common parameters used to estimate the thermal maturity of rock; nevertheless, some caution is needed in interpreting these data. The misidentification of primary vitrinite and solid bitumen, as well as the suppression of T_{max} and VR_r values, are issues to be considered to avoid misinterpretations of the thermal maturity [52].

The thermal maturity of the dispersed organic matter in Ramalhal-1 sediments was assessed by means of vitrinite reflectance, which is considered to be the most robust thermal maturity parameter for DOM (e.g., [1,9]). As shown in Figure 4A, there is a gradual increase in maturity through the Jurassic with a good correlation ($R^2 = 0.95$) between huminite/vitrinite reflectance and depth. Based on the conventional maturity threshold ("oil window" between 0.5–0.6% and 1.3%VR_r) [1,12,53], among others, Abadia-Lourinhã samples are in an immature-to-early-mature stage, while Brenha and Montejunto samples are mature.
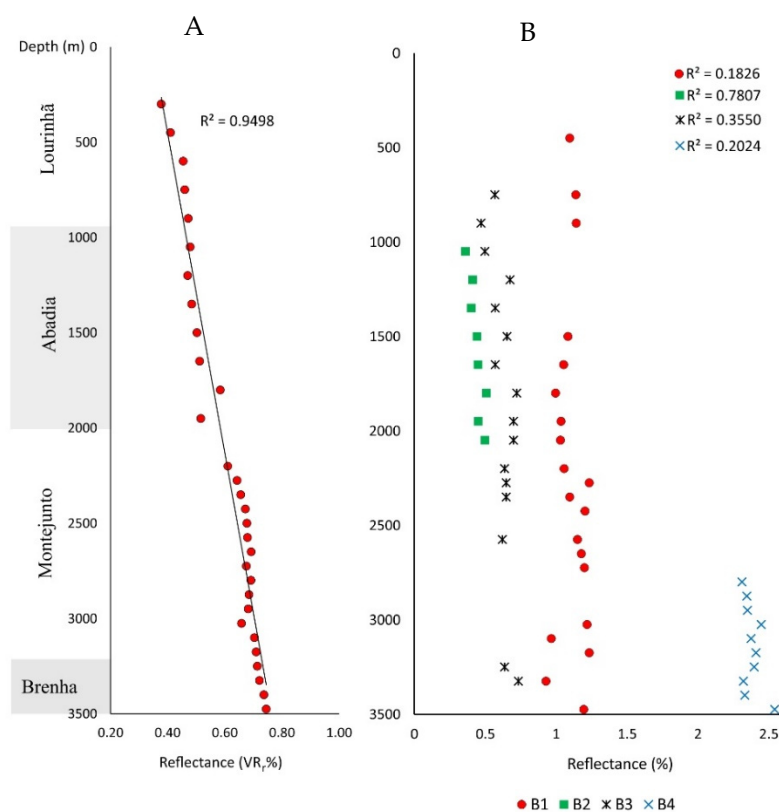

Figure 4. Mean random reflectance versus depth profile for Ramlhal-1 samples. (**A**) Huminite/vitrinite reflectance; (**B**) solid bitumen and pyrobitumen reflectances.

As referred to previously, Gonçalves et al. [6] attempted to use geochemical data (Rock-Eval pyrolysis data and biomarker ratios) as maturity indicators for samples from Ramalhal-1. These data pointed to an immature to mature OM stage; nevertheless, those data were not considered robust enough to be used as maturity parameters for the Ramalhal-1 sequence. One of the problems identified by the authors was the extremely low S2 values (pyrolysis data), which commonly provide unreliable T_{max} values [12,54]. Low S2 values can result from the interplay between several different factors. The presence of type III and IV kerogens usually shows a low or lack of S2 peak, respectively [55]. Additionally, rocks with TOC values < 0.5 wt.% typically present low S2 values, in the range of 0.0 to 2.5 mgHC/g.rock [12]. In addition, the presence of multi-populations of bitumen also interferes with the quality of T_{max} data, with values lower than the real thermal maturity

being expected [12]. The T_{max} data obtained by Gonçalves et al. [6] indicates that most of the samples were immature, which is not in agreement with the vitrinite reflectance data (Table 2) obtained in this study. As shown in Figure 5, the correlation of vitrinite reflectance and T_{max} values is very poor (R^2 = 0.18) and has no statistical significance, confirming that T_{max} cannot be used as an independent maturity indicator for the Ramalhal-1 samples.
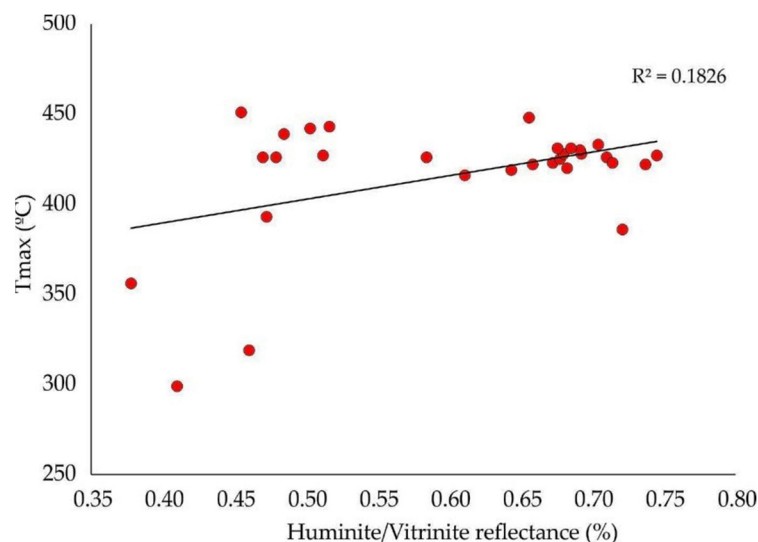

Figure 5. Huminite/vitrinite reflectance versus T_{max} plot for Ramalhal-1 well (T_{max} data from Gonçalves et al. [6]).

On the other hand, the biomarker ratios data are ambiguous, with some indicating a mature stage (e.g., M_{30}/H_{30} ratio, C32S/(S + R) hopanes) for the whole sequence, while others (e.g., C_{29} 20S/(20S + 20R) and C_{29} $\beta\beta/(\alpha\alpha + \beta\beta)$ steranes) point to an immature stage for the OM [6]. This discrepancy in the results can have several explanations, from diagenetic conditions, which can affect the biomarker data (e.g., [56,57]), to the presence of non-indigenous bitumens [58]. According to the literature (e.g., [59,60]), some solid bitumens are soluble or partially soluble in organic solvents, which makes the extracted bitumen a mixture of the bitumen generated in situ plus solid bitumen that may have migrated from other rocks. In these cases, biomarker ratios reflect not only the original OM characteristics, but also the migrated bitumen characteristics.

6.3. Relationship between Solid Bitumen and Huminite/Vitrinite Reflectance

Solid bitumen is frequently found in sedimentary basins worldwide, and the Lusitanian Basin is no exception. Recent studies have shown the presence of multi-populations of bitumen in the Lusitanian Basin, mainly in carbonated rocks, which are considered to have migrated from an unknown adjacent source rock [10,28].

In this study, four bitumen populations were differentiated due to their optical characteristics and, as mentioned above, some have features similar to those identified in previous studies [10,28]. Several works have proposed the classification of solid bitumen based on different characteristics, such as reflectance, solubility, chemical composition, etc. [46–48]. Following the terminology suggested by Mastalerz et al. [60], based only on bitumen reflectance, B1 to B3 populations can be classified as solid bitumen and the B4 population as pyrobitumen. A study published by Landis and Castaño [61] indicates that all bitumens with a reflectance above 0.7% should be classified as pyrobitumen; however, Mastalerz et al. [60] considered this value too low, and proposed 1.5%BR$_r$ as the boundary between solid bitumen and pyrobitumen, since at this reflectance value, much of the oil has already been cracked to gas, remaining only a residual insoluble bitumen (pyrobitumen). However, the same authors warned that care is needed when using these terms; for example, pyrobitumen can be observed in S-rich samples at a lower reflectance (1.2–1.3%BR$_r$).

As can be seen in Figure 4B and Table 2, the solid bitumen distribution along the Ramalhal-1 well was not uniform, with reflectance values ranging from 0.36% (B2) to 2.54% (B4). Only the B2 population reflectance values showed a slight correlation with depth, while all other bitumen populations maintained almost the same values across. For example, the high-reflecting bitumen (B4 pyrobitumen) keeps almost the same reflectance values for approximately 675 m. This fact may indicate the existence of multiple paths of hydrocarbon generation/migration in the Lusitanian Basin and/or neighbor basins. This trend was already described by Gonçalves et al. [28] for the three families of bitumen observed in samples from the Arruda sub-basin (Lusitanian Basin). This lack of linearity regarding the maturity of solid bitumens with depth was also reported by several authors, such as Gentzis and Goodarzi [62] for solid bitumen in the Permian and Lower Triassic interval record in Melville Island (Canada); by Petersen et al. [63] for bitumens in southern Scandinavia; and by Kus et al. [64] for the Upper Jurassic-Lower Cretaceous interval of the Chia Gara Formation (Kirkuk Oil Field, Iraq).

Bitumen reflectance is often used to estimate thermal maturity and is sometimes a supportive maturity parameter [60]. In sedimentary sequences where indigenous bitumen is present, bitumen reflectance is a robust parameter (e.g., [61,62,65,66]); nonetheless, its use can be further complicated in sequences where migrated bitumens are present, whereby the presence of multi-populations of bitumen is an obstacle to the use of solid bitumen reflectance as a maturity parameter. The literature suggests different approaches to select the bitumen population representing indigenous bitumen and, therefore, should be used to correlate with vitrinite. Jacob [59] recommended the selection of the bitumen with the lowest reflectance values, whereas others (e.g., [61,67]) preferred the bitumen population with the highest reflectance. Solid bitumens with a flat surface and without visible nanoporosity are better for reflectance measurements, according to Sanei et al. [68].

In this study, all the bitumen populations were selected for reflectance measurements and were compared with huminite/vitrinite reflectance. A lack of correlation between vitrinite and solid bitumen/pyrobitumen populations was observed (except for the B2 population, $R^2 = 0.80$; Figure 6), confirming that migration occurred, as already mentioned for solid bitumens in other parts of the Lusitanian Basin [10,28]. The correlation between huminite/vitrinite and B2 reflectances should be handled with caution since B2 solid bitumen was only observed in the Abadia Formation and the uppermost sample of the Montejunto Formation, which are at the beginning of catagenesis (vitrinite reflectance between 0.48% and 0.58%; Table 1). As referred to above, B2 solid bitumen has a viscous aspect (Figure 3A–C) and a yellow to brownish fluorescence color (Figure 3B). Solid bitumens produced in the early catagenesis stage are designated as "pre-oil solid bitumen" [69,70] or "initial-oil solid bitumen" [71] and result from the primary thermal cracking of the kerogen [69] and references therein. The relationship between vitrinite and B2 solid bitumen reflectances was established using the most common formulas [59,60,66] to calculate the vitrinite reflectance equivalent. The calculated values seem overestimated (see Supplementary Materials), being the mean difference between the measured and calculated reflectance ranging from 0.13% to 0.26%, depending on the equation used for the conversion. Considering this, the B2 solid bitumen seems to have migrated, similar to other bitumen populations. Given the above, bitumen reflectance should not be used to estimate the thermal maturity in this sub-basin and, as reported by Gonçalves et al. [28], nor in the adjacent Arruda sub-basin (Lusitanian Basin).
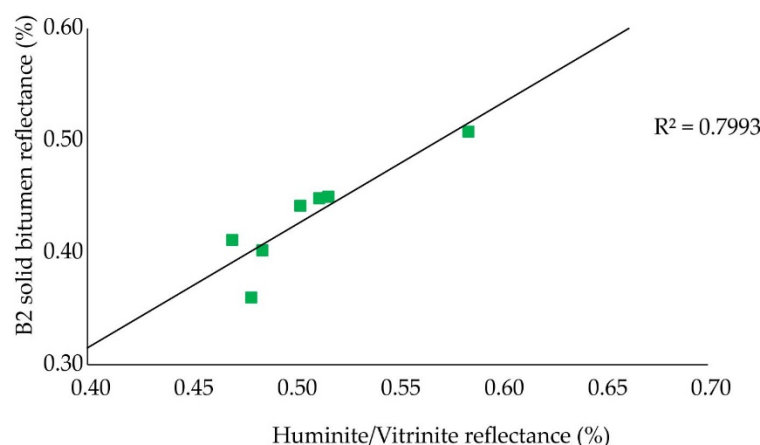
Figure 6. Correlation of vitrinite reflectance with the B2 solid bitumen reflectance from Ramalhal-1 samples.

7. Conclusions

Microscopic observations under reflected light of the DOM in samples from the Ramalhal-1 well were carried out, and the following conclusions were drawn:

- The Ramalhal-1 samples were poor in OM, mainly composed of inertinite, followed by sporinite and cutinite, relating to a type III-IV kerogen. The significant input of continental organic matter is indicative of a proximal depositional environment and corroborates the data from previous studies.

- Charcoal particles were identified mainly in the Kimmeridgian-Tithonian samples, evidencing the occurrence of wildfires near the depositional environment, possibly due to periods of hot and dry conditions.

- Four populations of bitumen co-existing in the same samples were recognized in this study. They were characterized based on their optical features, such as color in reflected and blue incident lights, surface texture and reflectance. Three were classified as solid bitumen, and the higher-reflectance bitumen was considered to be pyrobitumen.

- The thermal maturity assessment, based on huminite/vitrinite reflectance, showed that the DOM present in the samples from the Ramalhal-1 well were in an immature to mature stage.

- Reflectance data did not corroborate the maturity data obtained from geochemical data from a previous work. A lack of correlation was observed between T_{max} and huminite/vitrinite reflectance.

- Solid bitumen/pyrobitumen reflectance did not exhibit a linear correlation with either depth or huminite/vitrinite reflectance and cannot be used to assess thermal maturity.

- Organic petrology and organic geochemistry are complementary tools used to study DOM. Both techniques have limitations; however, for the Ramalhal-1 samples, organic petrology proved to be a better tool for assessing thermal maturity.

Author Contributions: Conceptualization, P.A.G.; methodology, P.A.G.; investigation, P.A.G.; resources, D.F.; writing-original draft preparation, P.A.G.; writing-review and editing, P.A.G., J.G.M.F. and D.F.; supervision, J.G.M.F. and D.F. All authors have read and agreed to the published version of the manuscript.

Data Availability Statement: The data presented in this study are available in the article.

Conflicts of Interest: The authors declare no conflict of interest.

References

1. Taylor, G.H.; Teichmüller, M.; Davis, A.; Diessel, C.F.K.; Littke, R.; Robert, P. *Organic Petrology*; Gebrüder Borntraeger: Berlin, Germany; Stuttgart, Germany, 1998; p. 704.
2. Tissot, B.; Welte, D.H. *Petroleum Formation and Occurrence*, 2nd ed.; Springer: Hidelberg, Germany, 1984; p. 540.
3. Tyson, R.V. *Sedimentary Organic Matter*; Chapman & Hall: London, UK, 1995; p. 615.
4. Fonseca, C.; Mendonça, J.O.; Mendonça Filho, J.G.; Lézin, C.; Duarte, L.V. Thermal Maturity Assessment Study of the Late Pliensbachian-Early Toarcian Organic-Rich Sediments in Southern France: Grands Causses, Quercy and Pyrenean Basins. *Mar. Pet. Geol.* **2018**, *91*, 338–349. [CrossRef]
5. Fonseca, C.; Mendonça Filho, J.G.; Lézin, C.; Duarte, L.V. Organic Facies Variability and Paleoenvironmental Changes on the Moroccan Atlantic Coast across the Cenomanian -Turonian Oceanic Anoxic Event (OAE2). *Int. J. Coal Geol.* **2020**, *230*, 103587. [CrossRef]
6. Gonçalves, P.A.; Mendonça Filho, J.G.; Mendonça, J.O.; da Silva, T.F.; Flores, D. Paleoenvironmental Characterization of a Jurassic Sequence on the Bombarral Sub-Basin (Lusitanian Basin, Portugal): Insights from Palynofacies and Organic Geochemistry. *Int. J. Coal Geol.* **2013**, *113*, 27–40. [CrossRef]
7. Gonçalves, P.A.; Mendonça Filho, J.G.; Silva, T.F.; Mendonça, J.O.; Flores, D. The Mesozoic-Cenozoic Organic Facies in the Lower Tagus Sub-Basin (Lusitanian Basin, Portugal): Palynofacies and Organic Geochemistry Approaches. *Mar. Pet. Geol.* **2014**, *52*, 42–56. [CrossRef]
8. Gonçalves, P.A.; Mendonça Filho, J.G.; Silva, T.F.; Flores, D. Palynofacies and Source Rock Potential of Jurassic Sequences on the Arruda Sub-Basin (Lusitanian Basin, Portugal). *Mar. Pet. Geol.* **2015**, *59*, 575–592. [CrossRef]
9. Suárez-Ruiz, I.; Flores, D.; Mendonça Filho, J.G.; Hackley, P.C. Review and Update of the Applications of Organic Petrology: Part 1, Geological Applications. *Int. J. Coal Geol.* **2012**, *99*, 54–112. [CrossRef]
10. Pereira, J.L.; Gonçalves, P.A.; Mendonça Filho, J.G.; Flores, D. The Vale Das Fontes Formation in the Alcobaça Area (Lusitanian Basin, Portugal): Organic Petrology Characterization and Thermal Maturation. *Comun. Geológicas* **2014**, *101*, 533–536.
11. Poças Ribeiro, N.; Mendonça Filho, J.G.; Duarte, L.V.; Silva, R.L.; Mendonça, J.O.; Silva, T.F. Palynofacies and Organic Geochemistry of the Sinemurian Carbonate Deposits in the Western Lusitanian Basin (Portugal): Coimbra and Água De Madeiros Formations. *Int. J. Coal Geol.* **2013**, *111*, 37–52. [CrossRef]
12. Peters, K.E.; Cassa, M.R. Applied Source Rock Geochemistry. In *The Petroleum System—From Source to Trap*; Magoon, L.B., Dow, W.G., Eds.; AAPG Memoir: Tulsa, OK, USA, 1994; Volume 60, pp. 93–120.
13. Kullberg, J.C.; Rocha, R.B.; Soares, A.F.; Rey, J.; Terrinha, P.; Callapez, P.; Martins, L. A Bacia Lusitaniana: Estratigrafia, Paleogeografia e Tectónica. In *Geologia De Portugal no Contexto Da Ibéria*; Dias, R., Araújo, A., Terrinha, P., Kullberg, J.C., Eds.; Universidade de Évora: Évora, Portugal, 2006; pp. 317–368.
14. Leinfelder, M.R.R.; Wilson, R.C.L. Seismic and Sedimentologic Features of Oxfordian-Kimmeridgian Syn-Rift Sediments on the Eastern Margin of the Lusitanian Basin. *Geol. Rundsch.* **1989**, *79*, 81–104. [CrossRef]
15. Wilson, R.C.L.; Hiscott, R.N.; Willis, M.G.; Gradstein, F.M. The Lusitanian Basin of West-Central Portugal: Mesozoic and Tertiary Tectonic, Stratigraphic and Subsidence History. *AAPG Bull.* **1989**, *46*, 341–362.
16. Montenat, C.; Guéry, F. L'intrusion Diapirique De Caldas Da Rainha et l'halocinèse Jurassique Sur La Marge Portugaise. *C. R. Acad. Sci. Paris* **1984**, *298*, 901–906.
17. Azerêdo, A.C.; Wright, V.P.; Ramalho, M.M. The Middle-Late Jurassic Forced Regression and Disconformity in Central Portugal: Eustatic, Tectonic and Climatic Effects on a Carbonate Ramp System. *Sedimentology* **2002**, *49*, 1339–1370. [CrossRef]
18. Rasmussen, E.S.; Lomholt, S.; Andersen, C.; Vejbæk, O.L. Aspects of the Structural Evolution of the Lusitanian Basin in Portugal and the Shelf and Slope Area Offshore Portugal. *Tectonophysics* **1998**, *300*, 199–225. [CrossRef]
19. Azerêdo, A.C.; Duarte, L.V.; Henriques, M.H.; Manuppella, G. *Da Dinâmica Continental no Triásico Aos Mares Do Jurássico Inferior e Médio. Cadernos de Geologia de Portugal*; Instituto Geológico e Mineiro: Lisboa, Portugal, 2003; p. 43.
20. Duarte, L.V.; Soares, A.F. Litoestratigrafia Das Séries Margo-Calcárias Do Jurássico Inferior Da Bacia Lusitânica (Portugal). *Comun. do Inst. Geológico e Min.* **2002**, *89*, 115–134.
21. ASTM D2797-11a. *Standard Practice for Preparing Coal Samples for Microscopical Analysis by Reflected Light*; ASTM International: West Conshohocken, PA, USA, 2011.
22. ASTM D 7708. *Standard Test Method for Microscopical Determination of the Reflectance of Vitrinite Dispersed in Sedimentary Rocks*; ASTM International: West Conshohocken, PA, USA, 2014.
23. International Committee for Coal and Organic Petrology (ICCP). The New Vitrinite Classification (ICCP System 1994). *Fuel* **1998**, *77*, 349–358. [CrossRef]
24. International Committee for Coal and Petrology. The New Inertinite Classification (ICCP System 1994). *Fuel* **2001**, *80*, 459–471. [CrossRef]
25. Pickel, W.; Kus, J.; Flores, D.; Kalaitzidis, S.; Christanis, K.; Cardott, B.J.; Misz-Kennan, M.; Rodrigues, S.; Hentschel, A.; Hámor-Vidó, M.; et al. Classification of Liptinite-ICCP System 1994. *Int. J. Coal Geol.* **2017**, *169*, 40–61. [CrossRef]

26. Sýkorová, I.; Pickel, W.; Christanis, K.; Wolf, M.; Taylor, G.H.; Flores, D. Classification of Huminite-ICCP System 1994. *Int. J. Coal Geol.* **2005**, *62*, 85–106. [CrossRef]

27. Flores, D.; Suárez-Ruiz, I. Organic Petrology in the Study of Dispersed Organic Matter. In *The Role of Organic Petrology in the Exploration of Conventional and Unconventional Hydrocarbon Systems*, 1st ed.; Suárez-Ruiz, I., Mendonça Filho, J.G., Eds.; Bentham Science: Sharjah, United Arab Emirates, 2017; Volume 1, pp. 34–76.

28. Gonçalves, P.A.; Mendonça Filho, J.G.; Silva, F.S.; Flores, D. Reprint of "Solid Bitumen Occurrences in the Arruda Sub-Basin (Lusitanian Basin, Portugal): Petrographic Features". *Int. J. Coal Geol.* **2015**, *139*, 217–227. [CrossRef]

29. Scott, A.C. Charcoal Recognition, Taphonomy and Uses in Palaeoenvironmental analysis. *Palaeogeogr. Palaeoclimatol. Palaeoecol.* **2010**, *291*, 11–39. [CrossRef]

30. Scott, A.C.; Glasspool, I.J. Observations and Experiments on the Origin and Formation of Inertinite Group Macerals. *Int. J. Coal Geol.* **2007**, *70*, 53–66. [CrossRef]

31. Lenton, T.M. The Role of Plants, Phosphorus Weathering and Fire in the Rise and Regulation of Atmospheric Oxygen. *Glob. Chang. Biol.* **2001**, *7*, 613–629. [CrossRef]

32. Chaloner, W.G. Fossil Charcoal as an Indicator of Palaeoatmospheric Oxygen Level. *J. Geol. Soc.* **1989**, *146*, 171–174. [CrossRef]

33. Berner, R.A. Phanerozoic Atmospheric Oxygen: New Results Using the Geocarbsulf Model. *Am. J. Sci.* **2009**, *309*, 603606. [CrossRef]

34. Uhl, D.; Jasper, A.; Schweigert, G. Charcoal in the Late Jurassic (Kimmeridgian) of Western and Central Europe–Palaeoclimatic and Palaeoenvironmental Significance. *Palaeobiodivers. Palaeoenviron.* **2012**, *92*, 329–341. [CrossRef]

35. Belcher, C.M.; McElwain, J.C. Limits for Combustion in Low O_2 Redefine Paleoatmospheric Predictions for the Mesozoic. *Science* **2008**, *321*, 1197–1200. [CrossRef]

36. Jones, R.B.; McCourt, C.B.; Morley, C.; King, K. Maceral and Rank Influences on the Morphology of Coal Char. *Fuel* **1985**, *64*, 1460–1467. [CrossRef]

37. Kwiecinska, B.; Petersen, H.I. Graphite, Semi-Graphite, Natural Coke, and Natural Char Classification–ICCP System. *Int. J. Coal Geol.* **2004**, *57*, 99–116. [CrossRef]

38. Suárez-Ruiz, I.; Flores, D.; Marques, M.M.; Martinez-Tarazona, M.R.; Pis, J.; Rubiera, F. Geochemistry, Mineralogy and Technological Properties of Coals from Rio Maior (Portugal) and Peñarroya (Spain) Basins. *Int. J. Coal Geol.* **2006**, *67*, 171–190. [CrossRef]

39. Omodeo-Salé, S.; Suárez-Ruiz, I.; Arribas, J.; Mas, R.; Martínez, L.; Herrero, M.J. Characterization of the Source Rocks of a Paleo-Petroleum System (Cameros Basin) Based on Organic Matter Petrology and Geochemical Analyses. *Mar. Pet. Geol.* **2016**, *71*, 271–287. [CrossRef]

40. Moura, H.; Suárez-Ruiz, I.; Marques, M.M.; Ribeiro, J.; Cunha, P.P.; Flores, D. Influence of Magmatic Fluids on the Organic and Inorganic Fractions of Coals from the Penarroya-Belmez-Espiel Basin (Spain). *Int. J. Coal Geol.* **2021**, *235*, 103679. [CrossRef]

41. Degani-Schmidt, I.; Guerra-Sommer, M.; Mendonça, J.O.; Mendonça Filho, J.G.; Jasper, A.; Cazzulo-Klepzig, M.; Iannuzzi, R. Charcoalified Logs as Evidence of Hypautochthonous/Autochthonous Wildfire Events in a Peat-Forming Environment from the Permian of Southern Paraná Basin (Brazil). *Int. J. Coal Geol.* **2015**, *146*, 55–67. [CrossRef]

42. Glasspool, I.J.; Scott, A.C. Phanerozoic Concentrations of Atmospheric Oxygen Reconstructed from Sedimentary Charcoal. *Nat. Geosci.* **2010**, *3*, 627–630. [CrossRef]

43. Mateus, O.; Dinis, J.; Cunha, P.P. The Lourinhã Formation: The Upper Jurassic to Lowermost Cretaceous of the Lusitanian Basin, Portugal–ladscapes Where Dinosaurs Walked. *Ciências Da Terra* **2017**, *19*, 75–97. [CrossRef]

44. Costa, A.; Flores, D.; Suárez-Ruiz, I.; Pevida, C.; Rubiera, F.; Iglesias, M.J. The Importance of Thermal Behavior and Petrographic Composition for Understanding the Characteristics of a Portuguese Perhydrous Jurassic coal. *Int. J. Coal Geol.* **2010**, *84*, 237–247. [CrossRef]

45. Suárez-Ruiz, I.; Jiménez, A.; Iglesias, M.J.; Laggoun-Defarge, F.; Prado, J.G. Influence of the Resinite on Huminite Properties. *Energy Fuels* **1994**, *8*, 1417–1424. [CrossRef]

46. Suárez-Ruiz, I.; Iglesias, M.J.; Jiménez, A.; Laggoun-Défarge, F.; Prado, J.G. Petrographic and Geochemical Anomalies Detected in the Spanish Jurassic Jet. In *Vitrinite Reflectance as a Maturity Parameter*; Mukhopadhyay, P.K., Dow, W.G., Eds.; Applications and Limitations, ACS Symposium Series; American Chemical Society: Chicago, IL, USA, 1994; pp. 76–92.

47. Gentzis, T.; Goodarzi, F. Reflectance Suppression in Some Cretaceous Coals from Alberta, Canada. In *Vitrinite Reflectance as a Maturity Parameter*; Mukhopadhyay, P.K., Dow, W.G., Eds.; Applications and Limitations, American Chemical Society Symposium Series; American Chemical Society: Chicago, IL, USA, 1994; pp. 93–110.

48. Hutton, A.; Cook, A.C. Influence of Alginite on the Reflectance of Vitrinite from Joadja, N.S.W., and Some Other Coals and Oil Shales Containing Alginite. *Fuel* **1980**, *59*, 711–714. [CrossRef]

49. Kalkreuth, W. Rank and Petrographic Composition of Selected Jurassic-Lower Cretaceous Coals of British Columbia, Canada. *Bull. Can. Pet. Geol.* **1982**, *30*, 112–139. [CrossRef]

50. Stach, E.; Mackowsky, M.-Th.; Teichmüller, M.; Taylor, G.H.; Chandra, D.; Teichmüller, R. *Stach's Textbook of Coal Petrology*, 3rd ed.; Gebrüder Borntraeger: Berlin, Germany; Stuttgart, Germany, 1982.

51. Suárez-Ruiz, I.; Prado, J.G. Characterization of Jurassic Black Shales from Asturias (Northern Spain): Evolution and Petroleum Potential. In *Composition, Geochemistry and Conversion of Oil Shales*; Snape, C., Ed.; Kluwer Academic: Dordrecht, The Netherlands, 1995; pp. 387–393.

52. Carvajal-Ortiz, H.; Gentzis, T. Critical Considerations When Assessing Hydrocarbon Plays Using Rock-Eval Pyrolysis and Organic Petrology Data: Data Quality Revised. *Int. J. Coal Geol.* **2015**, *152*, 113–122. [CrossRef]
53. Hunt, J.M. *Petroleum Geochemistry and Geology*; Freeman: San Francisco, CA, USA, 1996.
54. Yang, S.; Horsfield, B. Critical Review of the Uncertainty of T_{max} in Revealing the Thermal Maturity of Organic Matter in Sedimentary Rocks. *Int. J. Coal Geol.* **2020**, *225*, 103500. [CrossRef]
55. Peters, K.E. Guidelines for Evaluating Petroleum Source Rock Using Programmed Pyrolysis. *AAPG Bull.* **1986**, *70*, 318–329. [CrossRef]
56. Ten Haven, H.L.; DeLeeuw, J.W.; Peakman, T.M.; Maxwell, J.R. Anomalies in Steroid and Hopanoid Maturity Indices. *Geochim. Cosmochim. Acta* **1986**, *53*, 3073–3079. [CrossRef]
57. Peters, K.E.; Walters, C.C.; Moldowan, J.M. *The Biomarker Guide, Volume 2, Biomarkers and Isotopes in Petroleum Exploration and Earth History*, 2nd ed.; Cambridge University Press: London, UK, 2005.
58. Waples, D.W.; Machihara, T. *Biomarkers for Geologists: A Practical Guide to the Application of Steranes and Triterpanes in Petroleum Geology*; Series 9; AAPG, Methods in Exploration: Tulsa, OK, USA, 1991.
59. Jacob, H. Classification, Structure, Genesis and Practical Importance of Natural Solid oil Bitumen ("Migrabitumen"). *Int. J. Coal Geol.* **1989**, *11*, 65–79. [CrossRef]
60. Mastalerz, M.; Drobniak, A.; Stankiewicz, A.B. Origin, Properties, and Implications of Solid Bitumen in Source-Rock Reservoirs: A Review. *Int. J. Coal Geol.* **2018**, *195*, 14–36. [CrossRef]
61. Landis, C.R.; Castaño, J.R. Maturation and Bulk Chemical Properties of a Suite of Solid Hydrocarbons. *Org. Geochem.* **1995**, *22*, 137–149. [CrossRef]
62. Gentzis, T.; Goodarzi, F. A Review of the Use of Bitumen Reflectance in Hydrocarbon Exploration with Examples from Melville Island, Arctic Canada. In *Applications of Thermal Maturity Studies to Energy Exploration*; Nuccio, V.F., Barker, C.E., Eds.; SEPM: Tulsa, OK, USA, 1990; pp. 23–36.
63. Petersen, H.I.; Schovsbo, N.H.; Nielsen, A.T. Reflectance Measurements of Zooclasts and Solid Bitumen in Lower Paleozoic Shales, Southern Scandinavia: Correlation to Vitrinite Reflectance. *Int. J. Coal Geol.* **2013**, *114*, 1–18. [CrossRef]
64. Kus, J.; Khanaqa, P.; Mohialdeen, I.M.J.; Kaufhould, S.; Babies, H.G.; Meßner, J.; Blumenberg, M. Solid Bitumen, Bituminite and Thermal Maturity of the Upper Jurassic-Lower Cretaceous Chia Gara Formation, Kirkuk Oil Field, Zagros Fold Belt, Kurdistan, Iraq. *Int. J. Coal Geol.* **2016**, *165*, 28–48. [CrossRef]
65. Mukhopadhyay, P.K. Vitrinite Reflectance as Maturity Parameter: Petrographic and Molecular Characterization and Its Application to Basin Modelling. In *Vitrinite Reflectance as a Maturity Parameter: Application and Limitations*; Mukhopadhyay, P.K., Dow, W.G., Eds.; American Chemical Society Symposium Series: Washington, DC, USA, 1994; pp. 1–24.
66. Schoenherr, J.; Littke, R.; Urai, J.L.; Kukla, P.A.; Rawahi, Z. Polyphase Thermal Evolution in the Infra-Cambrian Ara Group (South Oman Salt Basin) as Deduced by Maturity of Solid Reservoir Bitumen. *Org. Geochem.* **2007**, *38*, 1293–1318. [CrossRef]
67. Hackley, P.C.; Araujo, C.V.; Borrego, A.G.; Bouzinos, A.; Cardott, B.J.; Carvajal-Ortiz, H.; Cely, M.R.L.; Chabalala, V.; Crosdale, P.J.; Demchuk, T.D.; et al. Testing Reproducibility of Vitrinite and Solid Bitumen Reflectance Measurements in North American Unconventional Source-Rock Reservoir Petroleum Systems. *Mar. Pet. Geol.* **2020**, *114*, 104172. [CrossRef]
68. Sanei, H.; Haeri-Ardakani, O.; Wood, J.M.; Curtis, M.E. Effects of Nanoporosity and Surface Imperfections on Solid Bitumens Reflectance (Br) Measurements in Unconventional Reservoirs. *Int. J. Coal Geol.* **2015**, *138*, 95–102. [CrossRef]
69. Curiale, J.A. Origin of Solid Bitumen, with Emphasis on Biological Marker Results. *Org. Geochem.* **1986**, *10*, 559–580. [CrossRef]
70. Hackley, P.C.; Brett, J.V.; Hatcherian, J.J. On the Petrographic Distinction of Bituminite from Solid Bitumen in Immature to Early Mature Source Rocks. *Int. J. Coal Geol.* **2018**, *196*, 232–245. [CrossRef]
71. Sanei, H. Genesis of Solid Bitumen. *Sci. Rep.* **2020**, *10*, 15595. [CrossRef] [PubMed]